IEEE Access
Multidisciplinary | Rapid Review | Open Access Journal

Received March 23, 2022, accepted April 12, 2022, date of publication May 12, 2022, date of current version May 27, 2022.

Digital Object Identifier 10.1109/ACCESS.2022.3174549

Apples and Oranges: On How to Measure Node Centrality in Payment Channel Networks

LUIS E. OLEAS-CHÁVEZ[1], CRISTINA PÉREZ-SOLÀ[2,3], AND JORDI HERRERA-JOANCOMARTÍ[1,3]

[1]Department of Information Engineering and Communications, Universitat Autònoma de Barcelona (UAB), 08193 Barcelona, Spain
[2]Internet Interdisciplinary Institute (IN3), Universitat Oberta de Catalunya, 08035 Barcelona, Spain
[3]Center for Cybersecurity Research of Catalonia (CYBERCAT), 08860 Barcelona, Spain

Corresponding author: Luis E. Oleas-Chávez (luis.oleas@autonoma.cat)

This work was supported in part by the Spanish Government under Grant RTI2018-095094-B-C22 "CONSENT."

ABSTRACT The Bitcoin Lightning Network (LN) disrupts the scenario as a fast and scalable method to make payment transactions off-chain, alongside the Bitcoin network, thereby reducing the on-chain burden. Understanding the topology of the LN is crucial, not only because it is key to performance, but also for ensuring its security and privacy guarantees. The topology of the LN affects, among others, the ability to successfully route payments between nodes, its resilience (against both attacks and random failures), and the privacy of payments. Existing research on LN topology focuses on studying the degree, betweenness, and closeness as metrics that better describe the centrality of nodes. However, to the best of our knowledge, previous studies do not encompass the network as a whole because of the limitation of using only the capacity of channels as its principal property. The contributions of this study are two-fold. On the one hand, this paper discusses the application of classic centrality metrics for evaluating the centrality in the LN. On the other hand, we provide alternative metrics to evaluate centrality. Our approach extends the analysis by adding metrics (strength, Opsahl, current-flow betweenness) and network properties (capacity, fee, balance, channel, and pending Hashed Timelock Contracts (HTLCs)). Based on the results obtained using these metrics, we provide an in-depth analysis of the metric that best defines the centrality of this network.

INDEX TERMS Bitcoin lightning network, blockchain, centrality metrics, multigraph, network topology, node centrality, path restrictions, payment channel network.

I. INTRODUCTION

Blockchain-based cryptocurrencies address double-spending problem by storing all transaction history in an immutable ledger, blockchain, to account for ownership of each coin or balance. Such an approach has its obvious scalability problems pointed out from its beginning [7], [8] and multiple solutions have been proposed. From all of them, two-layer approaches are nowadays one of the most used ones. Such solutions use an upper layer approach constructed over blockchain-based technology. One of those proposals is the Payment Channel Networks (PCN), a network that routes payments between users, being the LN over Bitcoin, the most used PCN at present.

Payment channels build PCN by linking pairs of users on the network. An untrusted mechanism, used by the underlying blockchain, allows establishing a channel that connects each pair of users. For instance, Bitcoin LN establishes its channels using a funding transaction that locks channel funds in a multisignature address controlled by both channel members. Since network users may open multiple channels with multiple users, the result is a P2P network of payment channels. Furthermore, PCNs allow the interesting property of payment atomic execution through multiple hops. Such property allows routing a payment between users A and B even if those users are not directly connected by a payment channel. The only need is that both users are linked through a payment path. The atomicity execution ensures that the multihop payment, although conceptually performed by multiple single payments between user pairs in the path, cannot be partially executed so in case one of the payment hops is executed the whole payments in the path will take place.

Having such a vision of PCN, the natural question that arises is to what extent the decentralization and untrusted model tied to the base blockchain layer have been extended

The associate editor coordinating the review of this manuscript and approving it for publication was Yilun Shang.

to those second layer proposals. To that end, measures on the centralization of PCN, such as the Bitcoin LN, has been published in multiple works [3], [11], [14], [17], [18], [24], [25]. However, as we point out in Section VII, most of those approaches do not capture the semantics of the PCN itself and only provide the first-level analysis of standard centrality measures of graph theory.

In this paper, we analyze different centrality measures of the Bitcoin LN both from a theoretical and from a practical point of view. We have chosen the Bitcoin LN to perform our practical analysis, although our theoretical approach can be applied to any PCN. We base our theoretical analysis on the very basic properties of the LN such as channel, capacity, balances, and fees. These properties can be directly identified in other PCN over which our model can be also applied. Our approach is novel in the sense that our analysis deepens into the semantics of the network properties that are specific to a PCN. Those related to channel capacity, channel balance, and payment processing fee.

The main contributions of the paper are:

1) We provide a general model for the LN, that takes into account not only the capacity of channels but also balances, fees, and other policy parameters.
2) We discuss the semantics of applying classical centrality metrics to evaluate the LN and explain how can they be used to evaluate LN properties. We also highlight important restrictions to take into account when evaluating the centrality of PCN.
3) We provide additional metrics to evaluate the centrality in the LN and explain why they are better suited for this purpose.
4) We analyze the centrality in the LN over a period of two years, using the model and semantics previously described.

The paper is organized as follows. In Section II we describe a model for the LN. This model is then used throughout the rest of the paper to represent LN instances. Then, Section III discusses the usage of classic centrality metrics to evaluate the centrality in the LN, highlighting the risks and pitfalls of doing so without taking into account the particularities of this network. After that, Section IV examines the concept of a path in the context of the LN and the consequences it has when computing centrality metrics. After the discussions, Section V summarizes the metrics we propose to use to evaluate the centrality in the LN, and Section VI provides the results of evaluating centrality over real LN snapshots. Section VII surveys the existing related work and finally, Section VIII presents the conclusions of the paper.

II. A MODEL FOR THE BITCOIN LN

Several literature papers (see Section VII for more details) model Bitcoin LN via graph theory tools. However, all the proposals reviewed are based mainly on very general information about the channels, such as their mere existence between two users and their capacity. But, they rule out other more subtle information that greatly affects the flow of money between users, such as: how both parts of the channel divide the capacity of a channel (i.e., their balance in the channel), or how the routing and HTLC apply the fees.

TABLE 1. Summary of the model's definition.

Graph	G_1	G_2
Notation	$G_1 = (V_1, E_1)$ $\overline{e}_{ij} = \overline{e}_{ji} = (\overline{v}_i, \overline{v}_j) = (\overline{v}_j, \overline{v}_i) \in E_1$	$G_2 = (V_2, E_2)$ $e_{ij} = (v_i, v_j) \in E_2$
Type	Undirected multigraph	Directed multidigraph
Data from	The blockchain	Off-chain transactions P2P messages
Nodes represent	Public keys	Public keys
Edges represent	Open channels	Current state of open channels
Edge identifier	Funding transaction outpoint	Funding transaction outpoint Source node PK
Edge properties	Capacity (c_{ij})	Available balance (b_{ij}) Blocked balance (h_{ij}) Fee per byte (f_{ij}) Minimum HTLC amount (m_{ij})

In this section, we propose a finer model to represent a snapshot[1] of the LN. We model the LN as two graphs G_1 and G_2, together with two functions, f_V and f_E, that map elements of one graph with elements of the other graph. G_1 is an undirected graph and G_2 is a directed graph. The rationale behind this decision is that there are properties of the channels that are better modeled with an undirected graph, but other properties are better represented with a directed one. Having thus two graphs, allows us to create a rich representation of the network. Moreover, this double representation allows us to apply graph-theoretic metrics to measure the nodes of the network in a significant way. Next, we describe the details of the two graphs that represent the LN using the proposed model, details summarized in Table 1.

Let $\mathbf{G_1} = (\mathbf{V_1}, \mathbf{E_1})$ be an **undirected** graph, that contains static channel information that can be extracted from the blockchain.

Nodes $\overline{v}_i \in V_1$ represent users of the LN identified by their public keys. Edges $\overline{e}_{ij} \in E_1$ represent open channels between those users. The outpoint (transaction identifier and output index) that funds the channel uniquely identifies each edge.

The graph G_1 may be a multigraph because many different channels can be opened between a pair of nodes. Moreover, the graph is indeed undirected, because the outpoint that defines is a 2-out-of-2 multisig output, where none of the two

[1] We define a snapshot of the LN as the status of the payment channels that conform the network at a given instant of time.

public keys has any advantage nor privileged position, and thus both participants have the same role in the relationship.

Edges encode channel information that can be extracted from the funding transaction, e.g., the capacity of the channel. We use the double subindex notation in an edge $\overline{e}_{ij}$ to indicate the index of each incident vertex of the edge, that is, $\overline{e}_{ij} = (\overline{v}_i, \overline{v}_j)$. Furthermore, since G_1 is an undirected graph, $\overline{e}_{ij} = \overline{e}_{ji} = (\overline{v}_i, \overline{v}_j) = (\overline{v}_j, \overline{v}_i)$. Note that, since G_1 is a multigraph, we add an index to identify the multiple edges of the same two nodes, $\overline{e}_{(ij)_k} = \overline{e}_{ijk}$. For simplicity, we omit this third index from the notation whenever it is not specifically needed. We denote by c_{ij} the capacity of edge $\overline{e}_{ij}$, with $c(\overline{e}_{ij}) = c_{ij}$.

Let $\mathbf{G_2} = (\mathbf{V_2}, \mathbf{E_2})$ be a **directed** graph, that contains dynamic channel information that is reflected in off-chain commitment transactions and P2P LN messages exchanged between nodes.

The set of nodes $v_i \in V_2$ represents public keys and is the same set of nodes of G_1, that is $V_2 = V_1$. The set of edges $e_{ij} \in E_2$ represents the current state of the channels between those public keys. Each edge is uniquely identified by the outpoint (transaction identifier and output index) that funds the channel and the source node they refer to. The graph G_2 may be a multidigraph because many different channels can be opened between a pair of nodes.[2]

Edges in E_2 encode more detailed information about the channel than data stored in the edges of E_1. The extraction of such information does not come from on-chain transactions but the commitment transactions exchanged from the LN nodes and also from the LN P2P messages that the nodes broadcast. Regarding commitment transactions, we can classify their outputs[3] in two types, depending on which of the two parties is the receiver. Therefore, we model each pair of commitment transactions as two directed edges: the edge $e_{ij} = (v_i, v_j)$ from v_i to v_j will encode v_i's balance in the channel and offered HTLCs and, reciprocally, the edge $e_{ji} = (v_j, v_i)$ from v_j to v_i will encode v_j's balance in the channel and offered HTLCs. We denote by b_{ij} the balance of edge e_{ij}, $b(e_{ij}) = b_{ij}$; and by h_{ij} the balance blocked in HTLC of edge e_{ij}, $h(e_{ij}) = h_{ij}$.

Furthermore, edges in E_2 also encode additional information extracted from channel policies sent within the LN P2P network, such as the fee that is charged to use the channel, f_{ij}, measured in satoshis per byte, and the minimum amount of satoshis that can be routed through that channel, m_{ij}.

Finally, we also define two functions, $\mathbf{f_V}$ and $\mathbf{f_E}$, for mapping nodes and edges between G_1 and G_2. Let $\mathbf{f_V} : \mathbf{V_2} \rightarrow \mathbf{V_1}$ be a bijective function that maps nodes of the graph G_2 with nodes of the graph G_1. Let $\mathbf{f_E} : \mathbf{E_2} \rightarrow \mathbf{E_1}$ be a noninjective surjective function that maps the edges of graph G_2 with the edges of graph G_1.

[2]Again, since G_2 is a multidigraph, we add an index to identify multiple edges of the same two nodes, $e_{(ij)_k} = e_{ijk}$. For simplicity, again, we omit this third index from the notation whenever it is not specifically needed.

[3]Commitment transactions have four types of outputs which are: local outputs, remote outputs, received HTLC, and offered HTLC.

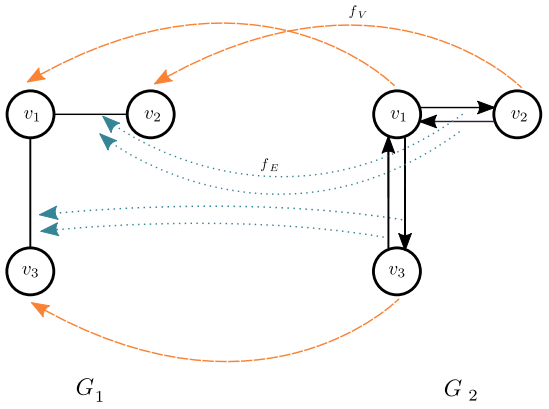

FIGURE 1. The data model.

Note that, regarding the defined model for the LN presented so far, the following restrictions must be preserved:

1) The set of nodes of both graphs is the same, that is, $V_1 = V_2$. So $\mathbf{f}_V$ is the identity function.
2) Each element $e \in E_2$ is mapped to exactly one element in E_1 (derived from the function definition).
   That is, for each $e_{ij} = (v_i, v_j) \in E_2$ with $f_V(v_i) = \overline{v}_i$ and $f_V(v_j) = \overline{v}_j$, there exists one edge $\overline{e}_{ij} = (\overline{v}_i, \overline{v}_j) \in E_1$.
3) Each element $\overline{e} \in E_1$ is the image of exactly two elements in E_2.
   That is, for each $\overline{e}_{ij} = (\overline{v}_i, \overline{v}_j) \in E_1$ with $f_V(\overline{v}_i) = v_i$ and $f_V(\overline{v}_j) = v_j$, there exists exactly two edges in E_2, e_{ij} and e_{ji}. Therefore, $|E_2| = 2 \cdot |E_1|$.
4) Let $e_{ij} = (v_i, v_j)$ and $e_{ji} = (v_j, v_i)$ be the edges of E_2, the balances and pending HTLC values must be consistent with the total capacity channel, so it must hold that:

$$b_{ij} + h_{ij} + b_{ji} + h_{ji} = c_{ij} = c_{ji}. \tag{1}$$

To sum up, Fig. 1 shows a toy example of an LN snapshot with 3 nodes and 2 channels using the proposed model.

III. A DISCUSSION ON CLASSIC CENTRALITY METRICS APPLIED TO LN NODES

In this section, we review different classical centrality measures proposed in the field of graph theory. As well, we analyze to what extent they preserve the centrality meaning when they are computed over a graph that models a payment network, like the LN.

A. SYMMETRIC GRAPHS

In his seminal paper laying the foundations of centrality metrics in social networks [9], Freeman used the star graph as a starting point to guide his exposition. In a star graph (Fig. 2), intuition leaves no doubt as to which node is more central. Furthermore, this node is not only the center point of the star graph, but also the most central position imaginable on any graph of a similar size order. But why is this node central? It has three structural properties: it has the highest degree (i.e., the most number of neighbors), it is in the shortest paths between other nodes, and its distance to other nodes

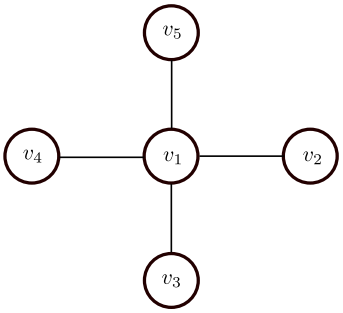

FIGURE 2. Basic star graph.

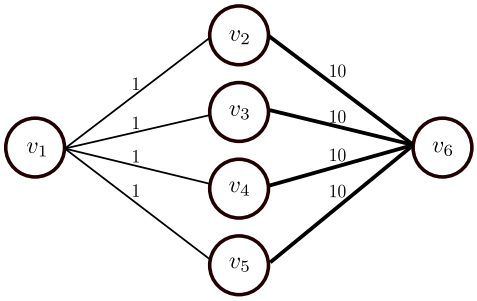

FIGURE 3. Weighted double star graph.

is minimal. These three properties are the basis of the three most basic centrality metrics for nodes in networks: degree, betweenness, and closeness centralities.

Given a graph of n nodes with adjacency matrix $A_{n\times n} = [a_{ij}]$, where a_{ij} is a binary value denoting whether there exists an edge between nodes v_i and v_j, degree centrality is defined as the number of neighbors of a node:

$$C_D(v_i) = \deg(v_i) = \sum_{j=1}^{n} a_{ij}. \tag{2}$$

The shortest path between two nodes is a path of the shortest length. Let σ_{st} be the number of the shortest paths between s and t; and $\sigma_{st}(v)$ the number of those paths that pass through v. Then, betweenness centrality is defined as the fraction of the shortest paths between all pairs of nodes of the graph that pass through v:

$$C_B(v) = \sum_{s\neq v\neq t\in V} \frac{\sigma_{st}(v)}{\sigma_{st}}. \tag{3}$$

The distance d between two nodes in a graph is the length of the shortest path between them. Closeness centrality is defined as the inverse of the sum of distances between one node and all the other nodes of the graph:

$$C_C(v_i) = \frac{1}{\sum_{j\in[1,n],j\neq i} d(v_i, v_j)}. \tag{4}$$

But to what extent are these centrality metrics relevant to evaluate nodes in the LN? Indeed, a node with a high **degree** is a node with lots of channels, which provides it with robustness (since it does not rely on a single or a few channels to be able to operate in the network). Moreover, a high degree also implies direct channels with more other nodes in the network and thus independence. On the other hand, a node with high **betweenness** is a node that is in the middle of payments between other nodes, in case the shortest path is used to choose payment routes. This allows it to have some degree of control and information about those payments (e.g., it knows the amount, HTLC values to estimate the overall number of hops, can decline participation, can delay payments), and also to obtain revenue from them in the form of fees. Finally, a node with high **closeness** may benefit from making payments with fewer hops, which may have consequences on both the fees to pay and the privacy of its payments.

B. SYMMETRIC WEIGHTED GRAPHS (CAPACITY)

However, these three basic metrics assume all channels are equally important (have the same contribution) to the importance of the node. Nonetheless, this is hardly the case: lightning channels have a capacity, that limits the amount of bitcoins a payment can move through them. For instance, take as an example the weighted double star graph shown in Fig. 3. To create it, one could just add v_6 to the simple star graph (Fig. 2) and connect it to v_2, v_3, v_4 and v_5; and where channels' capacity is represented as edge weights. Now, one could argue that node v_6 is more central than node v_1, since, although they both have exactly four channels and are in the same structural position on the graph, node v_6 can make payments of a higher amount in all of its channels.

Degree, betweenness, and closeness centralities have also been defined to take into consideration edge weights. Newman [20] and Barrat *et al.* [2] extends degree centrality to consider weights, where the **strength of a node** is defined as the sum of the weights of its connections (its incident edges):

$$C_D^w(v_i) = s(v_i) = \sum_{j=1}^{n} a_{ij} w_{ij}. \tag{5}$$

where w_{ij} is the weight of the edge between nodes v_i and v_j.

Brandes [5] and Newman [20] generalize the centralities of betweenness and closeness for weighted graphs using the sum of the weights of the edges of a path to define its length. Therefore, the shortest path between two nodes is not the path using the least number of hops, but the one that has the least sum of weights, and distance between nodes is defined in the same terms (i.e., the sum of weights of the edges in the shortest paths between them):

$$C_B^w(v) = \sum_{s\neq v\neq t\in V} \frac{\sigma_{st}^w(v)}{\sigma_{st}^w}, \tag{6}$$

$$C_C^w(v) = \frac{1}{\sum_{u\neq v\in V} d^w(v, u)} \tag{7}$$

TABLE 2. Centrality metrics for the weighted double star graph.

Nodes	C_D	C_B	C_C	C_D^w	C_B^w	C_C^w	$C_D^{1/w}$	$C_B^{1/w}$	$C_C^{1/w}$
v_1	4	3	0.83	4	6	0.33	4	0	0.98
$v_{2..5}$	2	0.25	0.625	11	0.25	0.29	1.1	0.25	2.94
v_6	4	3	0.83	40	0	0.09	0.4	6	3.3

where d^w and σ^w are distance and number of the shortest paths taking into account the sum of weights as the length of paths.

Getting back to our example (Fig. 3), node v_6 has now a higher weighted degree centrality (C_D^w) than node v_1 (40 and 4, respectively). Yet a problem arises when applying weighted betweenness (C_B^w) and closeness (C_C^w) centralities to evaluate the centrality of LN nodes. In their standard formulation, weight is interpreted as the cost of using that edge, whereas capacity is not the cost but the maximum amount that can be transacted through the channel. As a consequence, both betweenness and closeness centralities are higher for v_1 than for v_6, since all shortest paths between other nodes always pass through v_1, and v_1 has a lower distance to all other nodes in the graph. To circumvent this problem, some authors have used the multiplicative inverse of capacity as edges' weight [18] when computing betweenness and closeness centralities. With this definition, v_6 has now more weighted betweenness centrality than v_1 (6 and 0, respectively); and also higher weighted closeness (3.3 and 0.98, respectively), as shown in Table 2.

Again, it is important to understand what these metrics evaluate concerning LN nodes. Nodes with high **weighted degree** centrality are nodes that have a lot of capacity to operate within the network: they can potentially transact a higher amount. However, in contrast with unweighted high degree nodes, they will not always have strong robustness or independence, since C_D^w does not capture how this weight is distributed (i.e., it can be concentrated in a single channel). Section III-B1 explains how can we incorporate both the strength and the degree into the evaluation.

Note, also, that a node with high **weighted betweenness** centrality is a node that is in the middle of payments between other nodes that choose the shortest paths with higher capacities as payment routes. We argue that this is a very artificial use of the metric, that does not capture how payment networks operate. On the one hand, the restriction that only the path with the highest capacity (i.e., the lowest cost using the inverse of the capacity as weight) is going to be used does not make much sense in a payment network: any channel that has enough balance is valid, and the best path will be chosen based on other considerations such as fees. Sections III-D and III-E2 will explain how to deal with this. On the other hand, this does not take into account other restrictions in the routes, covered in Section IV.

Analogously, **weighted closeness** is again not very useful since it does not make sense to consider capacity as a cost or distance between nodes. Sections III-D will explain another approach that can better capture nodes' closeness.

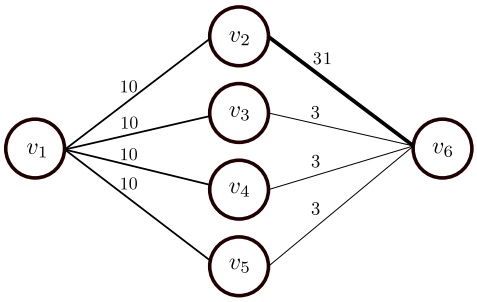

FIGURE 4. Example with two nodes with the same weight and strength.

1) WEIGHT AND STRENGTH

Node strength as defined in the previous section only takes into account the total engagement of the node, yet obliterates how is this involvement distributed across different connections. Therefore, although node strength is presented as a generalization of node degree for weighted networks, it fails to capture the original meaning of degree. Opsahl [22] *et al.* proposed a different formulation to combine both degree and strength:

$$C_D^{w\beta}(v_i) = deg(v_i)^{(1-\beta)} \cdot s(v_i)^{\beta} = C_D(v_i)^{(1-\beta)} \cdot C_D^w(v_i)^{\beta}. \tag{8}$$

This formulation depends on the parameter β to tune the contribution of the number of connections and the strength of the node into the centrality score: if β is 0, $C_D^{w\beta}$ is equal to the node degree; if β is 1, $C_D^{w\beta}$ is the node strength as defined by Newman; values of β between 0 and 1 provide higher $C_D^{w\beta}$ for nodes with a high degree, whereas values of $\beta > 1$ provide higher $C_D^{w\beta}$ for nodes with a lower degree.

However, when evaluating the robustness of a node or ability to make payments in the network, $C_D^{w\beta}$ still falls short. For instance, if we take a graph like the one shown in Fig. 4, nodes v_1 and v_6 have the same degree and strength. Consequently, regardless of the β value chosen, $C_D^{w\beta}$ is always the same for both nodes. However, intuitively node v_1 is better connected to the network, because of how its strength is distributed across its connections. An attack (or failure) of any of his channels would just affect 1/4 of its capacity. On the contrary, a directed attack over the v_2v_6 channel will strongly affect v_6, making him lose most of its capacity to operate with the network. A variant of the Opsahl metric can take this into account:

$$C_D^{w\alpha}(v_i) = \sum_{j=1}^{n} a_{ij} w_{ij}^{\alpha}. \tag{9}$$

This measure is indeed able to capture the differences between v_1 and v_6 (Table 3).

Again, if α is 0, $C_D^{w\alpha}$ is equal to the node degree; if α is 1, $C_D^{w\alpha}$ is the node strength as defined by Newman. For nodes with the same strength and degree, values of α between 0 and 1 provide higher $C_D^{w\alpha}$ for nodes with strength equally divided between channels, whereas values of $\alpha > 1$ provide higher

TABLE 3. Centrality metrics for the example graph (Fig. 4).

Nodes	C_D	s	$C_D^{w\beta}$						$C_D^{w\alpha}$					
			$\beta=0$	$\beta=1$	$\beta=0.25$	$\beta=0.9$	$\beta=0.95$	$\beta=1.25$	$\alpha=0$	$\alpha=1$	$\alpha=0.25$	$\alpha=0.9$	$\alpha=0.95$	$\alpha=1.25$
v_1	4	40	4	40	7.11	31.77	35.65	71.13	4	40	7.11	31.77	35.65	71.13
v_2	2	41	2	41	4.26	30.31	35.25	87.24	2	41	4.14	29.93	35.02	90.93
$v_{3..5}$	2	13	2	13	3.19	10.78	11.84	20.76	2	13	3.09	10.63	11.75	21.73
v_6	4	40	4	40	7.11	31.77	35.65	71.13	4	40	6.31	30.05	34.63	84.99

$C_D^{w\alpha}$ for nodes with strength concentrated in the same (or a small number of) channels (cf. v_1 and v_6).

C. DIRECTED WEIGHTED GRAPHS (BALANCE)

All the metrics presented so far are computed over the capacity of the nodes' channels, and thus provide information about the possible payments the node may be involved with. Taking into account the model presented in the previous section, all of them can be computed over graph G_1. However, they fail to capture another important detail of payment networks, the current balances of nodes in the channel. That is, at a certain instant of time, these measures do not take into account how is the capacity of the channel distributed between the two ends of the channel to evaluate its centrality. If we consider, for instance, the network from Fig. 4, the channel between v_1 and v_2 has a capacity of 10. However, the ability of both nodes to operate within the network will not be limited by this capacity, but by the balance that each of them has at that moment. If all the capacity is on v_2's side, v_1 will not be able to make payments (or route outgoing payments) through that channel, and thus its strength will be reduced from 40 to 30 (assuming he has all the possible balance in the other three channels).

Channel balances may be represented with a direct graph, where the weight of the edges represents the balance the source node has in a channel, which corresponds to graph G_2 of our model presented in the previous section. The sum of the two edges (one in each direction) that represent a channel is thus at most the capacity of that channel. Using this representation, we can use the directed versions of the metrics presented above to evaluate the centrality of a node.

Fig. 5 represents a possible distribution of balances for the network shown in Fig. 3. The edges with a balance of zero have not been drawn for readability. Most channels are completely unbalanced, with all the capacity available in just one direction. The exception is the channel between nodes v_2 and v_6, whose capacity is split equally between both nodes.

Degree-based centrality metrics over directed graphs distinguish between outgoing and incoming edges. For instance, indegree and outdegree (C_{D^-} and C_{D^+}, respectively) take into account the number of incoming or outgoing edges, respectively; and strength is also computed separately for incoming and outgoing edges. Metrics based on paths consider only those paths that are valid considering the direction of the edges.

Table 4 summarizes the centrality metrics for the directed graph example shown in Fig. 5.

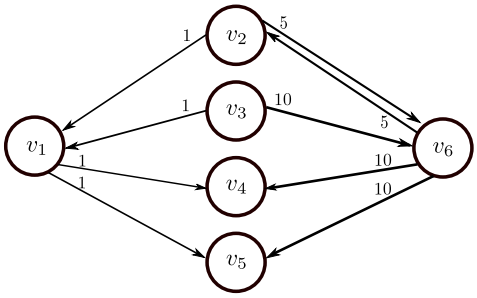

FIGURE 5. Directed double star graph.

TABLE 4. Centrality metrics for a directed weighted graph.

Nodes	C_{D+}	C_{D-}	C_B	C_C	C_{D+}^w	C_{D-}^w	C_B^w	C_C^w
v_1	2	2	2	0.75	2	2	6	0.37
v_2	1	2	1	0.67	5	6	3	0.1
v_3	0	2	0	0	0	11	0	0
$v_{4..5}$	2	0	0	0.67	11	0	0	0.33
v_6	2	3	3	1	15	25	1	0.13

D. SYMMETRIC WEIGHTED GRAPHS (FEE)

As we have seen in Section III-B, weighted betweenness and closeness centralities using capacity as weight are not able to capture the importance of a node, because these metrics are based on shortest paths and distances taking into account channel capacity as a cost.

Instead, using channel fees as weight is more representative of what rational nodes may implement since fees are indeed a cost of using the channel. Therefore, nodes with a high weighted betweenness centrality with fees as the weight will be in the middle of payments between other nodes that try to optimize the cost of their payments by choosing the cheapest routes. Moreover, nodes with a high weighted closeness centrality with fees as weigh will be nodes that can make payments with the lowest fees.

However, note that this approach, using a simple symmetric graph constructed by channels, has also a problem: channels can only be used if they have enough capacity and balance in the desired direction. Furthermore, dealing with payments in the LN, additional restrictions also apply, as we will explain in Section IV.

E. FLOW BASED CENTRALITY METRICS

One of the problems of using betweenness centrality as defined in the previous section is that it is based on shortest

paths. Even when considering weight, nodes that may offer connectivity to the network, but that are not found in the middle of these shortest paths are not considered to have any influence.

Let's consider again nodes v_1 and v_6 from 3 and note that betweenness centrality ($C_B^{1/w}$) is 0 for v_1 and 6 for v_6 (Table 2). These values may seem to indicate that node v_1 will never be in the middle of payments between other nodes. However, in a payment channel network, this may not be the case: with the information, we currently have in the graph, payments of less than or equal to 1 would have no reason to prefer to be routed through node v_6 over node v_1. Flow-based centrality metrics allow overcoming this limitation.

1) FLOW NETWORKS

Flow networks are used to model different problems, from pipes moving water to electrical or information networks.

A **flow network** is a directed graph that has a nonnegative capacity in each edge ($c : V \times V \to \mathcal{R}_{\geq 0}$). Nonexistent edges are assumed to have a capacity of 0. A flow network has two special nodes: a source s and a sink t.

A **flow** is defined in a flow network as a function that assigns a real number f to each pair of nodes ($f : V \times V \to \mathcal{R}_{\geq 0}$), such that:

1) for all $u, v \in V$, $0 \leq f(u, v) \leq c(u, v)$, and
2) for all $u \in V - \{s, t\}$, $\sum_{v \in V} f(v, u) = \sum_{v \in V} f(u, v)$.

That is, at each edge the flow f must be lower or equal than the capacity c (capacity constraint), and the flow must be preserved at each node except for the source and the sink (flow conservation constraint).

The **value** $|f|$ of a flow is:

$$|f| = \sum_{v \in V} f(s, v) - \sum_{v \in V} f(v, s). \tag{10}$$

Given a flow network, a source, and a sink, the **maximum-flow** problem consists in finding flow f of maximum value $|f|$. Let f'_{st} be a flow of maximum value between nodes s and t. Let $f'_{st}(v)$ be a flow of maximum value between nodes s and t passing through node v.

2) BETWEENNESS CENTRALITY BASED ON FLOW

Freeman [10] extended the betweenness centrality metric based on flow, where a node is more central to the extent where more flow between pairs of other nodes in the graph depends on it. That is, to define the flow centrality of a node v is through the amount of flow between any pair of nodes in the graph that needs to pass through v divided by the sum of the maximum flow values of any pair of nodes in the graph:

$$C_F(v) = \frac{\sum_{s \neq v \neq t \in V} |f'|_{st}(v)}{\sum_{s \neq v \neq t \in V} |f'|_{st}}. \tag{11}$$

Table 5 shows the flow centrality measure for the example graph from Fig. 3. In contrast with traditional betweenness centrality measures based on weight and its inverse (C_B^w and $C_B^{1/w}$, respectively), flow based betweenness centrality (C_F) is able to capture the ability of nodes to be in the middle of payment paths. Node v_6 is more central than v_1, to the extent that payments between other pairs of nodes will be able to be of a higher amount than payments through v_1. However, node v_1 may still be in the middle of payments between other nodes, given that it has a tenth of the C_F of v_6. In contrast to $C_B^{1/w}$, where the node is not considered to be on the shortest paths and is therefore assigned a centrality of 0).

TABLE 5. Flow based centrality for the weighted double star graph.

Nodes	C_B^w	$C_B^{1/w}$	C_F
v_1	6.00	0.00	0.090909
$v_{2..5}$	0.25	0.25	0.048780
v_6	0.00	6.00	0.878049

Flow based betweenness centrality allows to measure the importance of a node in a payment network to the extent it is in the middle of payments between other pairs of nodes (and therefore collect metadata about those payments and potentially profit from them).

3) BETWEENNESS CENTRALITY BASED ON CURRENT FLOW

Brandes [6] proposes a centrality metric based on variations of betweenness and closeness, but with a different model in which information spreads efficiently similar to electrical current. The proposed metric overcomes the limitations related to execution times and space requirements that arise with computing large networks. Regardless of the approaches taken in flow betweenness, about including nongeodetic paths in a node's total score and measuring the amount of flow that passes through a node, its paths must be optimized to achieve their maximum value, and thus, solve real situations in which information moves randomly.

A similar approach taken by Newman [21] measures betweenness centrality based on random walks, same as current-flow betweenness (C_{CF}) which measures the portion of current flow that passes through a node v between all possible node pairs in the network. The C_{CF} of a node v can be defined as the amount of current that flows through a node averaged over all node pairs s and t. To be more specific, C_{CF} of a node v is the average of the current flow over all source-target pairs:

$$C_{CF}(v) = \frac{\sum_{s \neq t \in V} {I_V}^{(st)}}{\frac{1}{2}n(n-1)}. \tag{12}$$

where ${I_V}^{(st)}$ represents the current flow through a node v between source s and target t and $\frac{1}{2}n(n-1)$ is a normalizing constant.

Table 6 shows the current flow centrality measure for the example graph of Fig. 3. We compare again the traditional betweenness measures based on weight and its inverse, as well as, the flow betweenness. On the contrary, to the previous metrics, current flow based betweenness

TABLE 6. Current Flow based centrality for the weighted double star graph.

Nodes	C_B^w	$C_B^{1/w}$	C_F	C_{CF}
v_1	6.00	0.00	0.090909	0.818181
$v_{2..5}$	0.25	0.25	0.048780	1.000000
v_6	0.00	6.00	0.878049	8.181818

centrality (C_{CF}) captures the flow that passes through a node in the middle of payment paths. Similar to flow betweenness, node v_6 is more central than v_1, therefore the flow of payments between other pairs of nodes will be greater than payments through v_1. However, nodes v_2 to v_5 are even more central than v_1 because those nodes can process more flow than node v_1.

a: FLOW-BASED METRIC SELECTION

Luo [16] states that C_F and C_{CF} share a similar behavior for measuring the frequency of a node v among a couple of nodes s and t. However, these metrics differ in that C_F bases its calculation by comparing the maximum possible paths containing node v. Furthermore, this metric can be described as the proportion of the volume of flow that passes through v when the flow reaches the maximum value [1]. However, this metric might ignore paths that are central in the network when they are not crossed by any unit of flow for pairs of nodes s and t [15]. On the other hand, C_{CF} measures the frequency of a node v in a random-walk, a name that is also given to this metric [6], [19], between nodes s and t when calculating all paths existing between those nodes. Unlike C_{CF}, C_F is not a realistic metric since it only considers a small subset of possible paths between nodes. At the moment when we consider the complexity of both metrics, C_F can be calculated in time $\mathcal{O}(m^2n)$, instead, the complexity of C_{CF} is $\mathcal{O}((m+n)n^2)$ using matrix methods. This comparison indicates that the computation demand of C_{CF} is comparable to C_F. Therefore, based on the aforementioned, we select current-flow betweenness as a metric to obtain the frequency of a node that occurs on a path.

IV. CONNECTIVITY IN THE SCOPE OF A PAYMENT NETWORK

The edges between nodes and the paths that form those edges define connectivity in classical graph theory. A path in a graph is a sequence of incident edges such that neither vertices nor edges are repeated. Although not introduced explicitly, the paths are the basis of some of the centrality measures we have reviewed in the previous section, such as betweenness and closeness centrality.

However, such a basic definition of a path may not be suitable in the scope of a payment network like the LN, since not all paths defined in this simple manner are valid payment routes in the modeled payment network. There exist some additional restrictions for a path to be a valid payment route.

Therefore, to provide more accurate centrality measures for the modeled LN, we redefine the concept of a path. We define a **payment path** for an amount σ as a path with the following restrictions:

1) There is enough balance in all the channels to fulfill the payment.
2) The length of the path is smaller or equal to 20.
3) The number of existing HTLCs in each channel is less than 14.
4) The policies of the nodes in the path are compatible.
   a) There exists a set of timeouts for all HTLCs in the path that fulfill the conditions on the nodes' policies for all nodes in the path.
   b) The amount of payment is higher than the minimum ($\sigma > min\_htlc$).

Note that the first restriction is a general restriction of any payment network while the other ones are more specific to the current LN implementation and are extracted from its specifications. For restriction 2, we refer to BOLT 4 Section Packet-Structure. Instead, restrictions 3 and 4b refer to BOLT 2 Sections Adding an HTLC-Rationale and The *open_channel* Message respectively. Finally, for restriction 4a, it refers to BOLTs 2 and 7 Sections *cltv_expiry_delta* Selection and Recommendations for Routing respectively.

V. PROPOSED CENTRALITY MEASURES IN THE SCOPE OF LN

Once reviewed all possible centrality measures that can be directly computed on the graph that model the LN, either the symmetric one G_1 or the directed one G_2,[4] we now propose and justify which of them are suitable to measure the centrality of the nodes of the network and which is the property that such centrality measure provides, in terms of robustness/resilience or surveillance/control.

Table 7 summarizes all the metrics considered in the measures presented in Section VI. The first column of the table identifies the measure and the second one provides the exact formula used to compute such metric. The third column provides information about the graph over which the metric is computed. Note that some metrics may have a different meaning if computed on a symmetric (G_1) or a directed (G_2) graph. The Weight column indicates which parameter of the LN is selected as the weight for the calculation (in the case of a weighted metric).

The Restrictions column indicates which restrictions have been considered when applying some specific measures. Note that two clear sets appear when dealing with restrictions: measures based on direct connectivity (degree) and measures based on indirect connectivity (path). The restriction that we have taken into account for direct connectivity is the existence of the channel (so the corresponding edge in the graph) and whether or not such a channel is enabled in the policy information that the node broadcasts. Regarding measures using path connectivity, we have applied the concept of payment path defined in Section IV with the restrictions indicated. Finally, the last column of the table provides a brief description of the meaning of each measure.

[4] See Section II for the defined model

TABLE 7. Summary of the proposed centrality metrics.

Centrality measure	Definition	Graph	Weight	Restrictions	Evaluated LN property
Degree	$C_D(v_i) = \deg(v_i) = \sum_{j=1}^{n} a_{ij}$	G_1	$\emptyset$	Channels enabled	Number of channels.
Strength	$C_D^w(v_i) = s(v_i) = \sum_{j=1}^{n} a_{ij} w_{ij}$	G_1	c	Channels enabled	The potential capacity of the node to transact in the LN.
Incoming strength	$C_{D^-}^w(v_i) = \sum_{j=1}^{n} a_{ji} w_{ji}$	G_2	b	Channels enabled	The balance available to make payments in the LN. The maximum amount a node may send.
Outgoing strength	$C_{D^+}^w(v_i) = \sum_{j=1}^{n} a_{ij} w_{ij}$	G_2	b	Channels enabled	The balance available to receive payments in the LN. The maximum amount a node may receive.
Opsahl	$C_D^{w\alpha}(v_i) = \sum_{j=1}^{n} a_{ij} w_{ij}^{\alpha}$	G_1	c	Channels enabled	Potential resilience of the node: The maximum amount a node may transact and distribution of this amount across other nodes.
Incoming Opsahl	$C_{D^-}^{w\alpha}(v_i) = \sum_{j=1}^{n} a_{ij} w_{ij}^{\alpha}$	G_2	b	Channels enabled	Resilience of the node with respect to making payments (the amount a node may pay taking into account how is it distributed across its neighbors).
Outgoing Opsahl	$C_{D^+}^{w\alpha}(v_i) = \sum_{j=1}^{n} a_{ji} w_{ji}^{\alpha}$	G_2	b	Channels enabled	Resilience of the node with respect to receiving payments (the amount a node may receive taking into account how is it distributed across its neighbors).
Betweenness	$C_B(v) = \sum_{s \neq v \neq t \in V} \frac{\sigma_{st}(v)}{\sigma_{st}}$	G_2	$\emptyset$	Valid payment path	How often the node is in the middle of payments between nodes that choose the shortest routes (less number of hops). A node can obtain a potential income in fees and the collection of information on other payments.
Weighted betweenness (cap)	$C_B^w(v) = \sum_{s \neq v \neq t \in V} \frac{\sigma_{st}^w(v)}{\sigma_{st}^w}$	G_2	f	Valid payment path	How often the node is in the middle of payments between nodes that choose the cheapest routes (the lower amount of fees). A node can obtain a potential income in fees and the collection of information on other payments.
	$C_B^w(v) \Rightarrow C_B^w(v)_c$		c	Valid payment path	How often the node can potentially transact a higher amount. A node in the middle of payments between other nodes can choose the shortest paths with higher capacities.
Flow-based betweenness	$C_F(v) = \frac{\sum_{s \neq v \neq t \in V} \lvert f' \rvert_{st}(v)}{\sum_{s \neq v \neq t \in V} \lvert f' \rvert_{st}}$	G_2	c	Valid payment path	Amount of bitcoins the node is able to route for payments between other nodes of the network. Resilience to disconnection (See **Flow-based Metric Selection** III-E3a for details).
Current-flow betweenness	$C_{CF}(v) = \frac{\sum_{s \neq t \in V} I_V^{(st)}}{\frac{1}{2} n(n-1)}$	G_2	c	Valid payment path	The flow of bitcoins handled by the node through the payment route between other nodes on the network.
Closeness	$C_C(v_i) = \frac{1}{\sum_{j \in [1,n], j \neq i} d(v_i, v_j)}$	G_2	$\emptyset$	Valid payment path	How close is the node to other nodes in the network, if he chooses the shortest routes (the lower amount of hops). Less usage of third party nodes to interact (privacy and security).
Weighted closeness	$C_C^w(v) = \frac{1}{\sum_{u \neq v \in V} d^w(v,u)}$	G_2	f	Valid payment path	How close is the node to other nodes in the network, if he chooses the cheapest routes (least fees). Less usage of third party nodes to interact (privacy and security).

VI. MEASURING THE LN

The moment a pair of nodes open and, at some point, close a payment channel, these two transactions are the only ones added to the blockchain. In theory, the payer and the payee can send an unlimited number of transactions to each other without committing them to the blockchain. A payer may send such transactions with the aid of the global view of the PCN topology, which is the main input for the routing algorithm that requires one to be aware of the structure of the network. In consequence, each node has to gather routing information through broadcasting messages (channel_announcement and channel_update) through the peer-to-peer network.

Although the transmitted messages contain information such as channel capacity, fee, and signatures, they lack to disclose the channel's balance due to privacy reasons. This factor could incur in that a payment may fail due to the uncertainty that sufficient funds are available to route a transaction. However, the payer may attempt to send a payment a given number of times, in which one could be successful. To avoid such a failure of insufficient funds, especially on multihop payments, LN uses HTLC to ensure

balance security. Similarly, in case of a stuck payment, HTLC allows reverting it, by the expiration of the transaction time locks. However, to process HTLC, the nodes involved in payment must be online. Otherwise, funds locked could take place for some time, or even, in the worst case, the funds could be stolen by an adversary.

Based on the depiction of the LN model described in Section II and the description of restrictions in Section IV, we evaluate the results of the simulations obtained from the implemented metrics explained in Section III. Altogether, we analyze 12 metrics divided into 5 scopes (degree, strength, Opsahl, betweenness, and closeness) as described in Table 7. Likewise, based on their scope we apply specific restrictions as are enabled channels (degree, strength, and Opsahl) and valid payment path (betweenness and closeness).

Our goal is to draw conclusions regarding the evolution of the metrics over time, i.e., since its conceptualization, we want to know if LN has been prone to be more or less centralized. As well, since our approach makes use of restrictions on paths, it makes us wonder whether or not their use affects the results of the computations and if this is the case, how much error is injected. On the other hand, from the analysis of metrics as betweenness, we are interested to know the degree of error injected if normal betweenness is used, as well as if there are lots of differences between the results of the different metrics based on the rank correlation coefficient.

A. SNAPSHOTS, DATASET AND THE NETWORK

In order to make multihop payments, LN clients need to know the current state of the network, that is, which other nodes there exist, what channels do they maintain, and what are policies applicable to those channels. A **snapshot** of the LN is a graph representing the current state of the network from the point of view of a node.

Although a snapshot captures the composition of the network, its scope does not cover the totality of channels that might exist. The view of the network depends on the information that a node collects, and probably private channels between other pairs of nodes will not be reflected. Therefore, our analysis is limited to public channels since roughly 13.48% are private channels [13].

In this paper, we use a dataset of LN snapshots captured by Elias Rohrer [23], [24]. The dataset contains snapshots of the network every 6 hours, over a two-year period (from October 2018 to November 2020). For our analysis, we subsampled the dataset and selected one weekly snapshot. We omitted periods where data were corrupted. Moreover, whenever the snapshot represents a disconnected graph, we restrict our analysis to the biggest connected component (that always contains more than 99% of the nodes of the network). Table 8 summarizes the main properties of the selected snapshots.

The first consideration to take into account is related to the channels, which can be either enabled or disabled.

TABLE 8. Snapshots per month from Oct. 2018 to Nov. 2020.

Snapshots	Nodes	Channels	Disabled Channels (%)	Average degree	# of pairs of nodes with multiple channels
2018_10_31__12_00	1,548	7,146	2,296 (32.12%)	9.2326	304
2018_11_07__12_00	1,599	7,425	2,319 (31.23%)	9.2871	311
2019_01_23__12_00	2,348	14,383	4,258 (29.60%)	12.2513	759
2019_02_27__12_00	3,590	30,546	9,986 (32.69%)	17.0173	1,848
2019_03_20__12_00	2,555	15,863	5,441 (34.29%)	12.4172	896
2019_04_27__12_00	2,125	6,435	1,708 (26.54%)	6.0565	459
2019_07_31__12_00	5,696	37,246	15,530 (41.69%)	13.0779	2,608
2019_08_07__12_00	5,824	36,030	15,808 (43.87%)	12.3729	2,615
2019_08_28__12_00	5,912	36,288	15,283 (42.11%)	12.276	2,583
2019_09_25__12_00	5,948	36,077	14,346 (39.76%)	12.1308	2,470
2019_10_30__12_00	5,630	31,252	12,578 (40.24%)	11.102	2,065
2020_02_26__12_00	6,386	36,170	15,049 (41.60%)	11.3279	2,468
2020_03_25__12_00	6,568	35,976	14,928 (41.49%)	10.9549	2,478
2020_04_29__12_00	6,822	36,296	15,400 (42.42%)	10.6409	2,544
2020_05_13__12_00	5,523	20,187	9,674 (47.92%)	7.3102	1,379
2020_10_28__12_00	3,714	7,426	7,426 (100%)	3.9989	140
2020_11_07__12_00	3,693	7,388	7,388 (100%)	4.0011	136

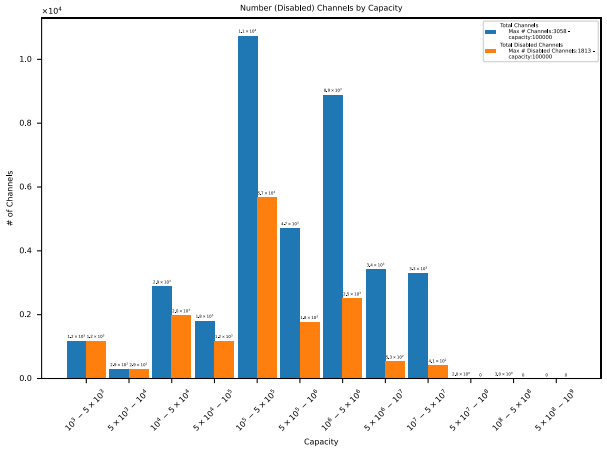

(a) Number of (disabled) channels between a pair of nodes by Capacity.

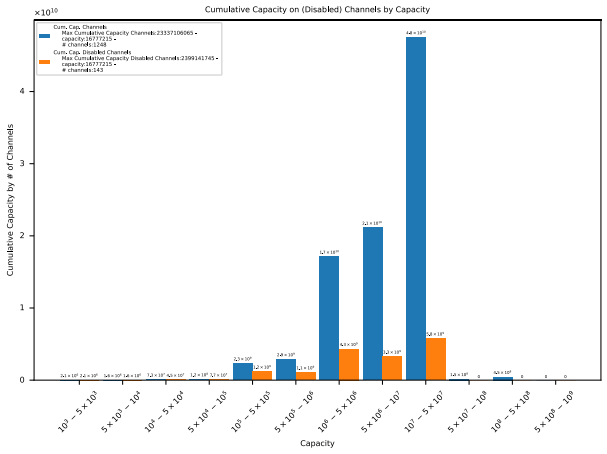

(b) Cumulative Capacity of (disabled) channels between a pair of nodes by Capacity.

FIGURE 6. Relationship between Pair of Nodes, Channels and Capacity.

We consider a channel to be disabled when either of the policies of both nodes in the channel is set to $disabled = True$ or the whole policy is set to $node\_policy = null$.

Fig. 6 shows the grouped distribution of the channels between pairs of nodes based on their capacities for the

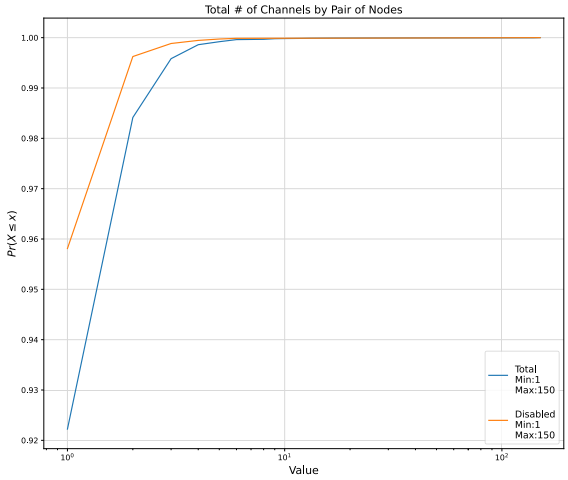

FIGURE 7. Number of channels between each pair of nodes.

snapshot corresponding to Jul. 31, 2019. For instance, Fig. 6(a) shows that there are $1.1 \cdot 10^4$ node pairs that created channels with capacities between 10^5 and $5 \cdot 10^5$ satoshis, of which $5.7 \cdot 10^3$ channels are disabled.

Even so, this range of channel capacities is not the one with the highest accumulated capacity among the channels. Fig. 6(b) shows that between 10^7 and $5 \cdot 10^7$ satoshis in channel capacities, there is a cumulative capacity of $4.8 \cdot 10^{10}$ of satoshis of which $5.8 \cdot 10^9$ satoshis are on disabled channels. Of this grouped distribution, $16.7 \cdot 10^9$ satoshis are the capacity setting that has the highest accumulated capacity with an amount of $23.3 \cdot 10^9$ between 1,248 pairs of nodes. Similarly, for that accumulated capacity, $2.3 \cdot 10^9$ remain among 143 disabled channels. These properties shape the LN topology that makes it peculiar, even more so, if we consider restrictions in the computation of the centrality metrics.

Another interesting property of the network is shown in the last column of Table 8, where it shows the number of pairs of nodes with more than one channel (multiple channels [4]). Fig. 7 shows the results of the aforementioned column, considering both the enabled and disabled channels for the snapshot with the highest number of channels (Jul. 31, 2019). Note that a vast majority of node pairs share at least one channel and a small percentage have two or more that correspond to hub nodes on the LN.

B. THE EFFECTS OF RESTRICTIONS ON CENTRALITY

As we explained in Section IV, not all paths on the LN graph can be used as payment paths. Therefore, additional restrictions must be considered to ensure that a given path can be used to make a payment on the LN. In this section, we provide the results of our experiments by calculating the centrality measures directly on the LN graph. Then, we compare these results with the same metrics calculated taking into account the restrictions on valid payment paths and enabled channels. Due to space constraints, results from one single snapshot (Sept. 4, 2019) are included. For the remaining snapshots, similar results were obtained in the analyzed graphs.

TABLE 9. Parameters for the simulations.

Restriction	Parameters	1^{st} simulation	2^{nd} simulation
0	channel flag	enabled	enabled
1	balance	-	10^5
2	max path	20	20
3	max HTLC	-	14
4a	HTLC timeout	-	valid payment
4b	min payment	-	10^5

As shown in Table 9, we run two different simulations to compute the centrality measures.

In the 1^{st} simulation, two general restrictions are considered that remain throughout the 2^{nd} simulation. On the one hand, to be able to use a channel in a payment path, the policies of both nodes in the channel must be configured as enabled (restriction 0 in Table 9). On the other hand, restriction 2 of Section IV indicates that payment paths cannot have more than 20 hops. Therefore, we use the value given in the LN specification for the routing protocol[5] [13]. Note that both restrictions are deterministic and enforced by standard LN payment protocols.

In the 2^{nd} simulation, we apply all restrictions defined in Section IV in which multiple parameters are defined. First of all, we set to $100k$ (10^5) satoshis the amount of the payment in our simulation, so the minimum balance needed in restriction 1 should be that value. Furthermore, as indicated above, we consider the limit of 20 hops for restriction 2. Regarding restriction 3, the LN specification for opening a channel[6] states that 483 is the limit for the number of pending HTLCs. Even though, we set the value of 14 as the limit for the number of HTLCs existing for each channel. Moreover, through a seed, we generate pseudo-random HTLCs, holding the same random generation for both simulations. This process is executed for each channel with its corresponding payment amounts and timeouts. The former reduces the balance in the channel until, at most, $balance = 0$. The latter increases for each channel the total timeout up to the upper limit given by *time_lock_delta*, which corresponds to the validation of restriction 4a. Finally, the minimum HTLC needed in restriction 4b is fixed to $\sigma = 10^5$.

Note that, in addition to these parameters defined for given restrictions, other values are needed in the payment network for the simulations. In particular, the balance of each node in the payment channel is required to decide whether a payment can be forwarded through that channel. Although for privacy reasons, channel balances are not publicly available, it has been proven that it is possible to learn channel balances executing any of the attacks already described in the literature [12]. However, for ethical reasons,

[5]See: *HopLimit* - https://github.com/lightningnetwork/lnd/blob/40d63d5b4e317a4acca2818f4d5257271d4ac2c7/routing/pathfind.go

[6]See: *max_accepted_htlcs* - https://github.com/lightningnetwork/lightning-rfc/blob/master/02-peer-protocol.md

we do not perform these attacks on the live network, so in both simulations, we generate the channel balances through a constant distribution, i.e., half the capacity is assigned to each side of the channel.

Even though we use the parameters of the simulations as a starting point to evaluate the network as a whole, we can indeed tweak such values to create different scenarios and therefore evaluate such a network to improve its payment algorithm. For instance, we can use average payment amounts expressed in satoshis for the restrictions 1 and 4b. We can consider one satoshi as the minimum interval, which is the default minimum HTLC given by the LN policy, and 10^5 satoshis as the maximum interval, since values above this interval have the highest failure rate for the payment path. This scenario can increase the number of nodes participating in payments, but can also be reduced by the fees charged for each hop in a payment path.

Similarly, we can obtain a varied engagement of the nodes in the network using distributions other than the constant for the balance, such as uniform, normal, exponential, or beta distributions. Such diverse assignations of the balance may describe a scenario closer to the network reality. Likewise, for restriction 4a, we can draw a scenario in which the timeouts increase on each pending HTLC. This modification affects the availability of channels for a payment path since it is constrained by *time_lock_delta*. These scenarios are an option to have a deeper analysis focused on improving the payments, but we limit the scope of our analysis.

In the next sections, we provide the results for each of the metrics, showing the cumulative distribution function (CDF) of the centrality values of all the nodes in the graph. We split the results into two different measures, degree-based measures and path-based measures, indicating both results for the 1^{st} and the 2^{nd} simulation.

1) DEGREE-BASED

Degree-based centrality measures are degree $C_D(v_i)$, strength $C_D^w(v_i)$, incoming strength $C_{D^-}^w(v_i)$, outgoing strength $C_{D^+}^w(v_i)$, Opsahl $C_D^{w\alpha}(v_i)$, incoming Opsahl $C_{D^-}^{w\alpha}(v_i)$ and outgoing Opsahl $C_{D^+}^{w\alpha}(v_i)$ (see Table 7 for details). The first three values can be measured over the modeled graph G_1 since such measures do not involve any edge direction of the graph. However, for incoming and outgoing measures of strength and Opsahl, G_2 needs to be used. Note that even when the pending HTLCs modify the channel balance, we get the same results for degree-based measures in both simulations. Since, although HTLCs reduce the capacity of the channel, this reduction only applies to metrics that consider incoming/outgoing values (balances), but not those that do not consider it (capacity). Consequently, even though the channel balance is essential at the time of payment, it is irrelevant in case the channel is disabled.

Regarding Node Degree, Fig. 8 contains the values of this metric that are the same for the 1^{st} and 2^{nd} simulations. As well, taking into account restrictions makes the network average degree goes down from 12.25 to 7.18, and the median

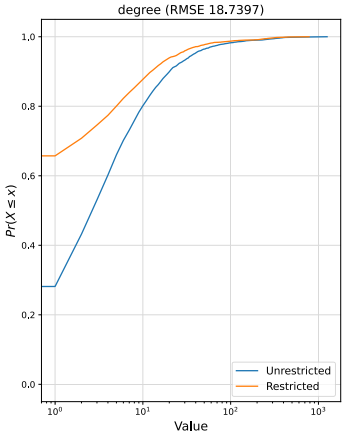

FIGURE 8. CDF - node degree, $C_D(v_i)$.

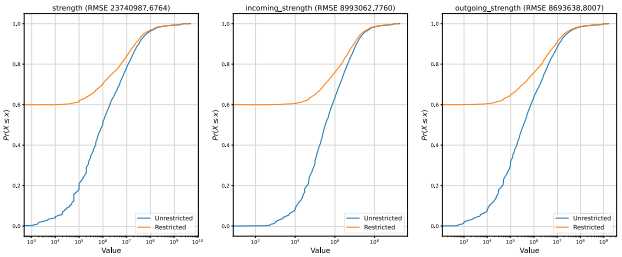

FIGURE 9. CDF - strength $C_D^w(v_i)$, incoming strength $C_{D^-}^w(v_i)$, outgoing strength $C_{D^+}^w(v_i)$ in both simulations.

from 3.0 to 0.0. The average RMSE of node's degree is 18.73. From the plot, we can observe that, when not taking into account restrictions, almost 50% of nodes are well-connected with 3 or more connections. However, such good connectivity is reduced to 30% of nodes when restrictions are considered. These differences are the result of a network with lots of channels disabled with 29,882 out of 72,274 channels which represent 41.34% disabled channels. As we review the remaining metrics, we will further explain this behavior in the next paragraphs.

Differences between restricted and unrestricted measures are also prominent when analyzing Strength and Opsahl metrics that derive from the capacity[7] of the channels. As shown in Fig. 9, average node strength has a reduction of 16.64% (from $28.54 \cdot 10^6$ to $23.79 \cdot 10^6$ satoshis), and the median of 100% (from $972 \cdot 10^3$ to 0 satoshis). Also, in Fig. 10, the reduction on average Opsahl centrality (for $\alpha = 0.5$) is 26.26% ($16.18 \cdot 10^3$ to $11.93 \cdot 10^3$ satoshis) and the median once again 100% ($1.67 \cdot 10^3$ to 0 satoshis). These differences are the result of 83.34% ($TotalUnrestrictedCapacity = 84, 173, 823, 510$ and $TotalRestrictedCapacity = 70, 158, 741, 106$) of the overall capacity is on enabled channels.

[7]Units are expressed in satoshis as such measurements are derived from channel capacity.

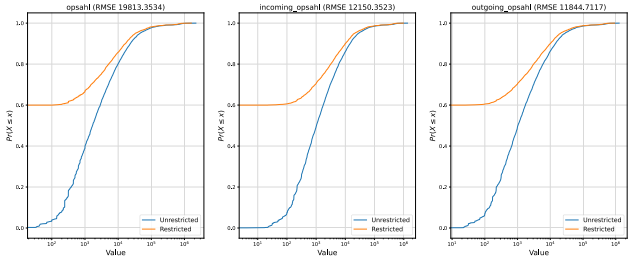

FIGURE 10. CDF - Opsahl $C_D^{w\alpha}(v_i)$, incoming Opsahl $C_{D^-}^{w\alpha}(v_i)$ and outgoing Opsahl $C_{D^+}^{w\alpha}(v_i)$ in both simulations.

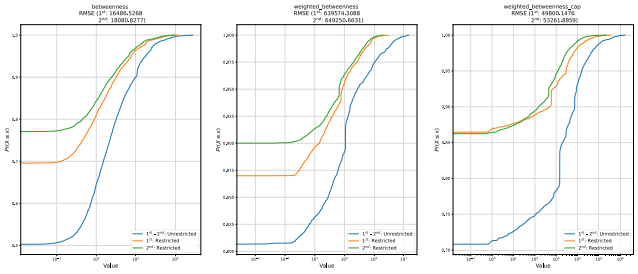

FIGURE 11. CDF - betweenness $C_B(v)$, weighted betweenness $C_B^w(v)$, weighted betweenness cap $C_B^w(v)_c$ and current flow betweenness $C_{CF}(v)$ of both simulations.

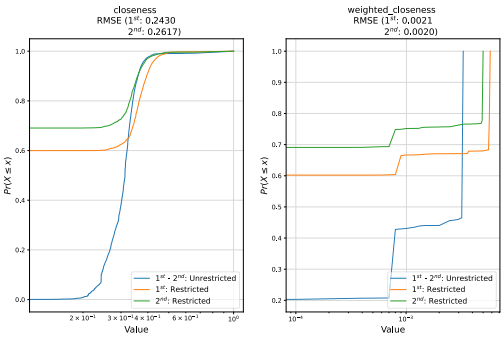

FIGURE 12. CDF - closeness $C_C(v_i)$ and weighted closeness $C_C^w(v)$ in both simulations.

2) PATH-BASED

Path-based centrality metrics are Betweenness $C_B(v)$, Weighted betweenness $C_B^w(v)$ and $C_B^w(v)_c$, Flow-based betweenness $C_F(v)$, Current-flow betweenness $C_{CF}(v)$, Closeness $C_C(v_i)$ and Weighted closeness $C_C^w(v)$ (see Table 7 for details). Note that all those metrics are computed using edge direction, so in our model definition and simulation they are computed over G_2. That means in the directed graph that represents the network with its balances, fees, and the blocked balance h_{ij} by the existing HTLCs. The total value h_{ij} for each channel and its timeout is randomly set through a seed that generates the same values for both simulations, which affects the balance of each side in the payment channel.

Fig. 11 and 12 show the results of each simulation for the betweenness and closeness centrality respectively with its variations as described previously in Table 7. At the moment, we compare the results of the metrics with weights for each simulation. There is a fluctuation in the values according to how the restrictions were used to compute the given metric. For instance, on the average ***betweenness*** for 1^{st} simulation, the reduction is 22.70%, however, this percentage compared with the 2^{st} simulation is 14.52%.

Instead, the average ***weighted_betweenness*** has values of 2.90% and 1.76% respectively, which shows a certain relationship given by the decrease in the balance because of existing HTLCs. On the contrary, for the average ***weighted_betweenness_cap*** which are 13.74% and 6.20% respectively, the aforementioned relationship does not last since the centrality measure has to consider paths with greater capacity to make a payment. Finally, the ***current_flow_betweenness*** metric has an average of 12.17% and 8.39% respectively, which when comparing its average ratio with ***weighted_betweenness*** metric, its results (1.45 and 1.57 respectively) are similar. Based on these results and the fact that betweenness indicates how much control has a node over the network, the centrality should be measured by a combination of factors such as: fee, capacity, and balance instead of relying on a unique property of the channel. Table 10 summarizes the values of both simulations for the betweenness centrality.

Subsequently, we took a similar approach with closeness metrics, as shown in Fig. 12, to determine how reachable is a specific node. Along with whether it would be the most central node in case it is located at a node distance from each other. For the ***closeness***, its average is 47.75% and 34.93% respectively, which follows a similar explanation about its marked difference due to the presence of existing HTLCs in the channels. On the other hand, for the ***weighted_closeness***, the average is around 100% and 50% respectively, in which, the results show almost a flat trend that could be due to the presence of nodes with a large degree, i.e., a given number of nodes are reachable quite easy. In any case and regardless of the specific metric used, restrictions heavily affect the results. This tendency determines that centrality has to be defined by not only one metric but for a set of them considering more than one property of the network. Table 11 summarizes the values of both simulations for closeness centrality.

C. RELEVANCE OF NODES ACCORDING TO CENTRALITY

Once we review the results of the metrics as a whole, it is appropriate to take a closer look at the most relevant nodes from the snapshot of Sept. 4, 2019. In doing so, we intend to find out how important some nodes on the network are to carry out payments either by the number of channels connecting them to the network or by the total capacity among those channels. For our analysis, we select five nodes. Four out of 5,897 nodes show high connectivity and *Bitrefill Thor* and *WalletOfSatoshi.com* are the pair of nodes with the most channels with 153 between them, none of which is disabled. On the other hand, the node that opened the most channels is *1ML.com node ALPHA* with 830 of which 400 are disabled. However, *LightningPowerUsers.com* is the node that has the most channels with 1,255 of which 473 are disabled. Finally,

TABLE 10. Betweenness centrality for 1^{st} and 2^{nd} simulations.

	1^{st} Simulation				2^{nd} Simulation			
	RMSE	Average		%	RMSE	Average		%
		Unrestricted	Restricted			Unrestricted	Restricted	
betweenness	16,486.5268	1,827.987	415.075	22.70%	18,080.8277	1,827.987	265.52	14.52%
weighted_betweenness	639,574.3088	53,515.367	1,553.671	2.90%	649,250.6631	53,515.367	944.274	1.76%
weighted_betweenness_cap	49,800.1476	6,797.366	934.270	13.74%	53,261.8859	6,797.366	421.803	6.20%
current_flow_based_betweenness	66,655.8598	15,290.226	1,861.887	12.17%	69,663.3386	15,290.226	1,283.072	8.39%

TABLE 11. Closeness centrality for 1^{st} and 2^{nd} simulations.

	1^{st} Simulation				2^{nd} Simulation			
	RMSE	Average		%	RMSE	Average		%
		Unrestricted	Restricted			Unrestricted	Restricted	
closeness	0.2430	0.312	0.149	47.75%	0.2617	0.312	0.109	34.93%
weighted_closeness	0.0021	0.002	0.002	100%	0.0020	0.002	0.001	50%

TABLE 12. Comparison of Degree, Strength & Opsahl Metrics between simulations.

Nodes	*degree*	*strength*	*Opsahl*
LightningPowerUsers.com	1255 (1^{st})	2,408,839,730 (6^{th})	1,738,704.6504 (2^{nd})
ACINQ	991 (3^{rd})	4,897,182,784 (1^{st})	2,202,977.1081 (1^{st})
1ML.com node ALPHA	884 (4^{th})	659,107,300 (55^{th})	763,315.6969 (24^{th})
WalletOfSatoshi.com	390 (17^{th})	1,302,003,973 (39^{th})	712,587.924 (34^{th})
Bitrefill Thor	248 (49^{th})	2,151,521,848 (12^{th})	730,463.8378 (30^{th})

ACINQ is the node with the highest capital distributed among its channels with $4.89 \cdot 10^9$ satoshis.

1) DEGREE-BASED

Table 12 shows, for the nodes mentioned above, the results and their positions within the degree-based metrics among the most relevant nodes. It is worth mentioning that these results come from G_1 where only the *enabled channel* restriction is considered. *LightningPowerUsers.com* has the highest degree, so it can be considered as the main ***hub***[8] in the network. Instead, *1ML.com node ALPHA* can be seen as a ***beacon***[9] since it has the most open channels with other nodes. Even though, its strength is the lowest compared to the other four nodes. Also, *ACINQ* has the highest *strength* among the nodes, which is one of the preferred metrics for analyzing a weighted network. This result could mean that this specific node has a high level of involvement in the network, although its degree is not the highest. Due to the greater number of channels connecting *WalletOfSatoshi.com* and *Bitrefill Thor*, we can assume this pair of nodes is a ***bridge***.[10] Although *WalletOfSatoshi.com* has a higher degree, it has a low strength compared to *Bitrefill Thor*. By analyzing Opsahl, which combines degree and strength with a tune parameter $\alpha = 0.5$, once again *LightningPowerUsers.com* has a relative importance in the network. Nevertheless, even without the highest degree, *ACINQ* is the node with both the highest strength and Opsahl. As a consequence, the importance of a node is not only due to the number of channels that connect it to its neighbors, but also due to its participation in the network.

2) PATH-BASED

On the other hand, Table 13 compiles the results and their positions within the path-based metrics for the same five nodes. Thus, we analyze them through the betweenness metrics, with restrictions on the *valid payment path* mentioned in Section IV. Overall, these metrics give us an idea of the extent to which a node participates in the transactions between other nodes. As well, it indicates that a node could control the network since its income is proportional to how central it is with respect to the payment route. Again, *LightningPowerUsers.com* is the one with the highest betweenness scores, the same as the degree metric. The importance of this node lies not only in its numerous connections but also in how it stands among its neighbors, which makes it a ***broker***.[11] Although *ACINQ* generates the highest fee income and has the greatest strength and Opsahl, it handles less capital compared to *LightningPowerUsers.com*. Besides, *1ML.com node ALPHA*, which has a low strength, its betweenness metrics results are quite higher compared to the bridge nodes. The reason could be because this node creates most of the channels that allow it to connect with the network without making mostly payments.

[8]Defined as a node that connects with many other nodes

[9]Defined as a node that handles information about the awareness of the network topology.

[10]Defined as a pair of nodes that create a tie between nodes that would otherwise be disabled to perform payments without a direct connection.

[11]Defined as the node that connects dispersed nodes in order to obtain a competitive advantage based on access to network information.

TABLE 13. Comparison of Betweenness Metrics between simulations.

Nodes	*betweenness*		*weigthed_betweenness*	
	1^{st} simulation	2^{nd} simulation	1^{st} simulation	2^{nd} simulation
LightningPowerUsers.com	151,899.0754 (1^{st})	92,033.136 (1^{st})	173,505.7543 (8^{th})	122,204.9509 (9^{th})
ACINQ	113,773.3293 (2^{nd})	61,115.5338 (2^{nd})	431,786.3497 (4^{th})	235,449.8886 (4^{th})
1ML.com node ALPHA	81,270.1248 (4^{th})	52,827.8882 (5^{th})	146,710.3616 (12^{th})	91,583.8489 (12^{th})
WalletOfSatoshi.com	14,280.1376 (44^{th})	8,043.7234 (49^{th})	15,986.7698 (93^{rd})	3,958.9318 (150^{th})
Bitrefill Thor	2,084.7293 (153^{rd})	2,164.2028 (114^{th})	13,509.6234 (103^{rd})	10,277.3408 (101^{st})
Nodes	*weighted_bettweenness_cap*		*current_flow_betweenness*	
	1^{st} simulation	2^{nd} simulation	1^{st} simulation	2^{nd} simulation
LightningPowerUsers.com	120,297.0834 (6^{th})	83,946.1151 (3^{rd})	310,126.8883 (1^{st})	216,591.8611 (1^{st})
ACINQ	60,987.8653 (18^{th})	44,310.7451 (8^{th})	274,519.0144 (2^{nd})	189,553.5902 (2^{nd})
1ML.com node ALPHA	189,272.5644 (3^{rd})	196,024.2667 (2^{nd})	128,011.6723 (13^{th})	93,000.8053 (10^{th})
WalletOfSatoshi.com	34,613.1407 (34^{th})	8,349.4167 (64^{th})	67,345.7153 (48^{th})	42,294.1871 (51^{st})
Bitrefill Thor	586.0000 (488^{th})	446.0000 (454^{th})	55,804.9380 (54^{th})	41,117.8770 (52^{nd})

TABLE 14. Comparison of Closeness Metrics between simulations.

Nodes	*closeness*		*weighted_closeness*	
	1^{st} simulation	2^{nd} simulation	1^{st} simulation	2^{nd} simulation
LightningPowerUsers.com	0.5418 (20^{th})	0.5080 (25^{th})	0.0058 (10^{th})	0.0050 (10^{th})
ACINQ	0.5286 (23^{rd})	0.5031 (26^{th})	0.0058 (15^{th})	0.0050 (15^{th})
1ML.com node ALPHA	0.4950 (42^{nd})	0.4475 (66^{th})	0.0058 (72^{nd})	0.0050 (78^{th})
Bitrefill Thor	0.4497 (119^{th})	0.4386 (79^{th})	0.0058 (237^{th})	0.0050 (242^{nd})
WalletOfSatoshi.com	0.4879 (52^{nd})	0.4702 (42^{nd})	0.0058 (291^{st})	0.0050 (299^{th})

On the contrary, when we compare the bridge nodes, the relevance of *Bitrefill Thor* decreases with respect to *WalletOfSatoshi.com*. This fact is more evident on the metric *weighted_betweenness_cap*, which means that *WalletOfSatoshi.com* has a higher capital distributed among its neighbors. As well, the revenue from fees charged by this node is slightly higher, which could mean that this node could be continuously chosen as a payment intermediary. Finally, the *current_flow_betweenness* metric restates the behavior seen so far. Nodes with a higher degree and betweenness, especially with *weighted_betweenness_cap*, have a higher probability to participate in payment routes, i.e., these nodes withstand a higher traffic load than most of their neighbors.

Lastly, Table 14 contains very similar results between the five nodes for the closeness metrics. Although, when we analyze *closeness* values, the *LightningPowerUsers.com* node keeps a higher centrality. It indicates that the node is well connected at a short distance from the other nodes and could efficiently distribute payments. Regarding the *weighted_closeness* metric, the results of the five nodes are the same, which means that each node applies the same fee. Therefore, they can be used to route payments without diminishing their centrality.

D. METRICS CORRELATION

The metrics that we propose are conceptually more suitable for measuring centrality in payment networks. However, these metrics have the drawback that they are computationally more expensive to calculate. In consequence, we are interested in observing the correlation between the metrics that we propose and other simpler ones. Since, if the correlation is high, then we can use the simplest ones as a proxy as long as there are computational restrictions. For that purpose, we use Spearman's rank correlation to determine the degree of association (strength and direction) of a monotonic relationship between two metrics. The value of the coefficient ranges from -1.00 to 1.00, depending on how the two variables are related, for the strongest negative and positive correlation, respectively. The sign of the coefficient corresponds to the direction of the relationship, i.e., if it is positive, one variable increases as the other tend to increase, meanwhile, if it is negative, one variable decreases as the other tends to increase.

For the first part of this analysis, we use the snapshot from Sept. 4, 2019, to compare the results of the metrics from the 1^{st} and 2^{nd} simulations. In addition, we decided to show the correlation coefficients of the metrics using a heat map, since it helps to visualize the variance between multiple metrics, show similarities between them as well as detect if there is any correlation between them. In Fig. 13, whose results are analogous to both simulations, there is a low-to-medium relationship between the betweenness metrics, which remains when compared to the degree metric. On the other hand, there is a strong relationship between *weighted_betweenness* and *weighted_betweenness_cap* metrics. In that case, the coefficient value is the same (0.62) among the results of both simulations, even though, in the 2^{nd} simulation: (1) the balance of the channels decreases because of the existing HTLCs and (2) the restrictions applied in the network.

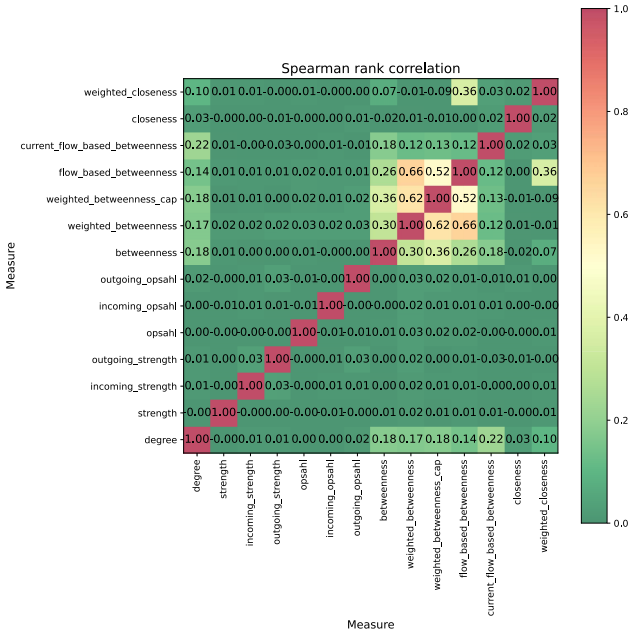

FIGURE 13. Similar metric correlation between 1st and 2 nd simulations.

For the last part of this analysis, and as mentioned above, the snapshot set used in our study covers data for the span of a couple of years. These data allow us to obtain a wide range of information to analyze. We compared the results of the 1st simulation between three snapshots since Oct. 2018, with a lapse of one year between the other two snapshots. Thus, we can infer, based on the results shown in Fig. 14, that the degree metric keeps a constant correlation with the metrics of *betweenness*, *weighted_betweenness* (capacity and fee), and *current_flow_betweenness*. For instance, on 2018 the strength of association of degree metric against these four betweenness metrics was 0.22, 0.21, 0.20, and 0.29 respectively, as well in 2020 the results kept slightly similar values 0.23, 0.23, 0.21, and 0.30 respectively.

Similarly, among these same four metrics hold a strong correlation compared with the remaining metrics. In fact, comparing the results between 2019 and 2020 shows that the relationship strengthens over time. For instance, in 2019, the relationship between betweenness and the metrics of weighted betweenness (fee and capacity) and current flow betweenness is 0.31, 0.35, and 0.17, respectively. The results of the same metrics increased for 2020 with values of 0.41, 0.44, and 0.26, respectively. Although, when we compare both weighted betweenness metrics (fee and capacity), these metrics keep an even stronger correlation, the highest value being 0.67 for them in 2020. As the LN structure adjusts over time, the correlation comparison between snapshots gradually decreases for the betweenness and closeness metrics. For instance, in the case of weighted betweenness (fee and capacity) in Oct. 2018 they maintained a degree of relationship between 0.51 and 0.46, respectively. By Oct. 2020 it was reduced to -0.04 and -0.11, respectively.

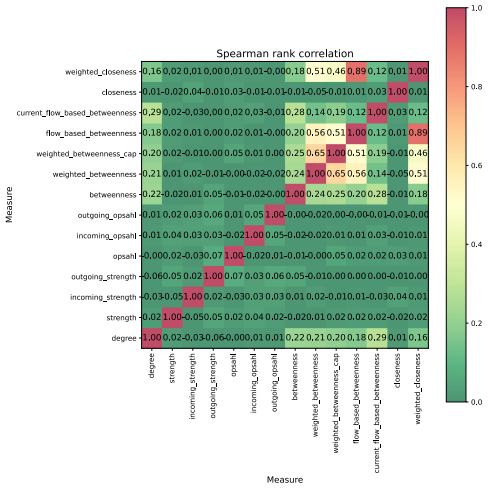

(a) Correlation Oct. 2018.

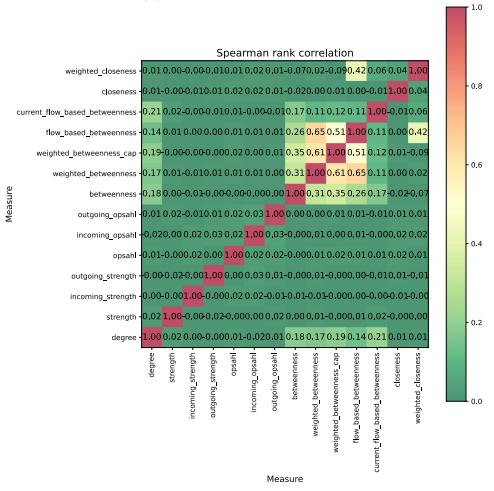

(b) Correlation Oct. 2019.

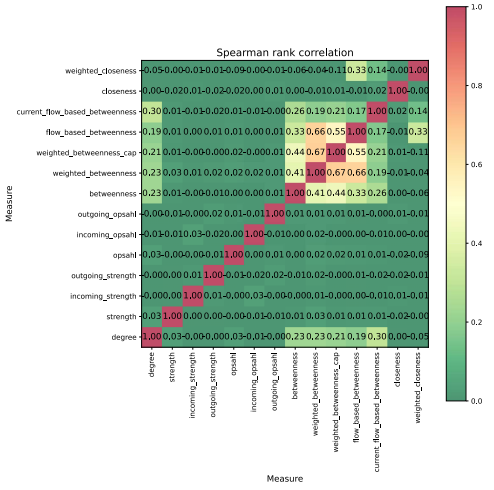

(c) Correlation Oct. 2020.

FIGURE 14. The correlation of metrics over a span of two years Oct. 2018 - 2020.

Based on these results, the main conclusion could emerge to explain the correlation of the centrality metrics. For a

TABLE 15. LN graph and metrics.

Research	Period	Nodes/Channels	Model for the LN	Metrics
[14]	18 snapshots (Jan18/Jul19)	8216/122517	• Weighted (capacity) undirected network • Number of nodes $N^{(t)}$ • Symmetric matrix $W^{(t)}$ • Capacity $s_i^{(t)}$ • Adjacency matrix $A^{(t)}$ • Number of open channels $L^{(t)}$ t:time snapshot	• Gini • Degree centrality • Closeness centrality • Betweenness centrality • Eigenvector centrality • Core-periphery structure
[17]	12 snapshots (Jan18/Jan19) mainnet	3613/23860	• Weighted (capacity) undirected network	• Median degree • Lower strength
[3]	40 snapshots (Dec17/May19)	4787/N-A The number of merchant nodes in the union of all 40 snapshots is 169.	• Undirected weighted multigraph	• Estimated income by traffic volume • Number of failed payments by node unavailable
[24]	Oct.–Nov/18 and Jan.–Feb/19	around 2500/N-A	• graph $G = (V, E)$, where V is the set of nodes and E the set of edges • subgraph $G = (V, E)$ where $V' \subseteq V$ and $E' \subseteq E$ is called a connected component	• Degree of a vertex $deg(v)$ • Distance and Diameter • Average path length • Betweenness • Small-world networks • Scale-free networks • Number of reachable nodes • Network's node cardinality • Average maximum flow. • Expected payment success ratio • Average fee gain
[11]	Apr18/Apr19	7796/41705	• Undirected weighted snapshot graph G • Weight: the biggest payment amount between two nodes at that time. • Edge weight: the sum of capacities of all the channels between the same two nodes. • Edge added if there is no edge between two nodes (Edge's weight: channel capacity)	• Assortativity coefficient • Effective eccentricity • Closeness • Betweenness • PageRank
[25]	Jan19	2344/16617	• Undirected weighted graph (capacity). Capacity: the sum of individual balances.	• Beetweenness • Closeness • Local clustering coefficient • Percolation threshold
[18]	12 snapshots Jan18/Jan19	4189/67917	• Undirected weighted (capacity) network	• Average local efficiency among all the nodes

given pair of metrics, the correlation values between different snapshots vary more than five percentage points from each other. However, these metrics can provide insight into the evolution and behavior of the network. This conclusion lies in its lack of dependence between one and the other metric, but they are also necessary because they do not have redundant information.

VII. RELATED WORK

Our work builds on prior research to expand the analysis of centrality measures, and thus, to get a deeper grasp of the semantics of Bitcoin LN properties. The period over which these works took place goes from as long as the one performed in [3] to a more concise one as in [25]. Additionally, research as [14], [17], [18], [25] modeled LN, through graph theory tools, from a general point of view by getting together basic data of channels such as: channel existence among users and its payment capacity. Regarding to the model used to depict LN, research [3], [11], [14], [18], [24], [25] represent the network as an undirected weighted graph. The weighted property employed on the analysis was the capacity, considering that funds on channels have an unknown distribution and channels' direction changes constantly. Table 15 outlines some studies that expose the network topology with their characteristics and attributes as well as some metrics. However, these proposals dismiss meaningful properties of the network related to channel capacity, the balance of each node that shares a channel and fees used for payment processing. From the set of proposals mentioned above, the model on [3] is the only one that depicts the graph as a multigraph, i.e., this model considers the probability that nodes may have multiple channels between

them. On top of that, [24] describes LN's topology on its simplest representation as a graph with nodes and channels without considering either weight or direction.

Based on these premises, we collect snapshots for a lapse of two years to evaluate the evolution of the network concerning centrality measures. As part of our research, we propose to model LN through G_1[12] and G_2[13] graphs. Each one encompasses the whole information of the network without leaving aside network characteristics that are essential at the time to comprehend the payment flow between buyers, sellers, and intermediate hops. Therefore, modeling of both multigraphs has to preserve the restrictions defined in Section II, since each one allows us to analyze this payment network in different contexts. Specifically, G_1 handles information related to LN properties such as: multiple channels between a pair of nodes that might or not be enabled to perform payments, and payment capacity. Similarly, G_2, besides those LN properties of G_1, handles information of channels such as balance, balance blocked in HTLC, and channel policies (fees and minimum payment amounts routed by the channel).

On the other hand, most researches provide highlights about the centrality measures such as degree [14], [17], [24], betweenness [11], [14], [24], [25] and closeness [11], [14], [25]. Also, some approaches [3], [17], [24] state the LN structure is best characterized by a centralized network, which is compatible with a core-periphery network [14]. In addition, each proposal attempts to determine the centrality metric that best defines this payment network, beyond the usual measures. For instance, [14] uses a core-periphery structure, [3] focuses on estimating the income by traffic volume and number of failed payments, [24] finds out the average maximum flow and the expected payment success ratio, and [18] determines the average local efficiency among all nodes. Nonetheless, they lack emphasis on LN properties that define more precisely the flow of satoshis between users, based on the fees that modify the payment capacity of the channel.

To the best of our knowledge, no proposal captures the relevant details of payment networks, since the reviewed works do not consider the distribution of balance, fees, blocked balance on HTLC, the minimum payment amount, and channel availability. These approaches only consider the channel capacity that may be involved with payment to evaluate its centrality.

VIII. CONCLUSION

In this paper, we study node centrality in the network of channels of the LN. To do so, we first provide a model for the network that incorporates many properties (such as balances, disabled channels, or fees) and restrictions (such as payment path lengths or minimum payment values) omitted in previous studies. We justify why these properties are relevant for studying centrality, and we propose a set of metrics to evaluate the node centrality in the context of payment channel networks. Finally, we use the proposed model and metrics to study the centrality of the LN for a period of two years.

Our results show that there are significant differences in the centrality values when these additional properties and restrictions are taken into account. Overall, the error injected into path-based metrics ranges from 1.14 to 12.82 percentage points. Although, for the weighted_closeness metric, its deviation is 50 percentage points due to a sizable reduction in the number of channels. On the other hand, when comparing normal betweenness against the other betweenness variations, the error injected by the first one is greater than the rest of the results. For instance, there are 7.04 (weighted_betweenness) and 0.64 (weighted_betweenness_cap) percentage points of difference with normal betweenness.

Some of the metrics we propose to use are computationally expensive to compute. Therefore, we also studied the correlation between different metrics to analyze if some metrics can be used as proxies for others. In our simulations, we found that the betweenness metrics hold a low-to-medium relationship, which is held when compared to the degree metric. Although, the strongest relationship belongs to weighted_betweenness and weighted_betweenness_cap. In contrast, throughout a couple of years of study, the degree metric holds a constant correlation with the betweenness metrics. But these same betweenness metrics have a strong correlation with each other, which gets stronger over time. Based on the different results, we can state that the computationally simple metrics can be used as intermediaries for the calculation of complex ones.

Finally, we can draw as the main conclusion that to provide a global understanding of the centrality in LN, we must consider most of the results of the metrics. We cannot rely on a single metric to define the centrality of the nodes, however, it is advisable to take the degree metric as a starting point. From there, we can analyze the network based on restrictions, its properties (fee, balance, existing HTLC, and enabled channels), or a combination of both.

[12]Undirected weighted multigraph with static channel information

[13]Directed weighted multigraph with dynamic channel information

REFERENCES

[1] T. Agryzkov, L. Tortosa, and J. F. Vicent, "A variant of the current flow betweenness centrality and its application in urban networks," *Appl. Math. Comput.*, vol. 347, pp. 600–615, Apr. 2019.
[2] A. Barrat, M. Barthélemy, R. Pastor-Satorras, and A. Vespignani, "The architecture of complex weighted networks," *Proc. Nat. Acad. Sci. USA*, vol. 101, no. 11, pp. 3747–3752, Mar. 2004.
[3] F. Beres, I. A. Seres, and A. A. Benczur, "A cryptoeconomic traffic analysis of Bitcoin's lightning network," 2019, *arXiv:1911.09432*.
[4] A. Biryukov, G. Naumenko, and S. Tikhomirov, "Analysis and probing of parallel channels in the lightning network," Cryptol. ePrint Arch., Univ. Luxembourg, Luxembourg, Tech. Rep. 2021/384, 2021.
[5] U. Brandes, "A faster algorithm for betweenness centrality," *J. Math. Sociol.*, vol. 25, no. 2, pp. 163–177, 2001.
[6] U. Brandes and D. Fleischer, "Centrality measures based on current flow," in *Proc. Annu. Symp. Theor. Aspects Comput. Sci.* Berlin, Germany: Springer, 2005, pp. 533–544.
[7] (2015). Cryddit. *Permanently Keeping the 1 MB (Anti-Spam) Restriction is a Great Idea*. Bitcointalk. [Online]. Available: https://bitcointalk.org/index.php?topic=946236.msg10388435#msg10388435.

[8] R. Financial. (2021). *How Bitcoin Can Scale*. River. [Online]. Available: https://river.com/learn/how-bitcoin-can-scale/
[9] L. C. Freeman, "Centrality in social networks conceptual clarification," *Soc. Netw.*, vol. 1, no. 3, pp. 215–239, 1978.
[10] L. C. Freeman, S. P. Borgatti, and D. R. White, "Centrality in valued graphs: A measure of betweenness based on network flow," *Social Netw.*, vol. 13, no. 2, pp. 141–154, Jun. 1991.
[11] Y. Guo, J. Tong, and C. Feng, "A measurement study of bitcoin lightning network," in *Proc. IEEE Int. Conf. Blockchain (Blockchain)*, Jul. 2019, pp. 202–211.
[12] J. Herrera-Joancomartí, G. Navarro-Arribas, A. Ranchal-Pedrosa, C. Pérez-Solà, and J. Garcia-Alfaro, "On the difficulty of hiding the balance of lightning network channels," in *Proc. ACM Asia Conf. Comput. Commun. Secur.*, New York, NY, USA, Jul. 2019, pp. 602–612.
[13] G. Kappos, H. Yousaf, A. Piotrowska, S. Kanjalkar, S. Delgado-Segura, A. Miller, and S. Meiklejohn, "An empirical analysis of privacy in the lightning network," 2020, *arXiv:2003.12470*.
[14] J.-H. Lin, K. Primicerio, T. Squartini, C. Decker, and C. J. Tessone, "Lightning network: A second path towards centralisation of the bitcoin economy," *New J. Phys.*, vol. 22, no. 8, Aug. 2020, Art. no. 083022.
[15] A. Lulli, L. Ricci, E. Carlini, and P. Dazzi, "Distributed current flow betweenness centrality," in *Proc. IEEE 9th Int. Conf. Self-Adaptive Self-Organizing Syst.*, Sep. 2015, pp. 71–80.
[16] Z. Luo, "Network research: Exploration of centrality measures and network flows using simulation studies," M.S. thesis, Univ. Twente, Enschede, The Netherlands, 2018.
[17] S. Martinazzi, "The evolution of lightning Network's topology during its first year and the influence over its core values," 2019, *arXiv:1902.07307*.
[18] S. Martinazzi and A. Flori, "The evolving topology of the lightning network: Centralization, efficiency, robustness, synchronization, and anonymity," *PLoS ONE*, vol. 15, no. 1, Jan. 2020, Art. no. e0225966.
[19] (2020). NetworkX. *Current Flow Betweenness centrality*. NetworkX Network Analysis in Python. [Online]. Available: https://networkx.org/documentation/stable/reference/algorithms/generated/networkx.algorithms.centrality.current_flow_betweenness_centrality.html#networkx.algorithms.centrality.current_flow_betweenness_centrality
[20] M. E. J. Newman, "Scientific collaboration networks. II. Shortest paths, weighted networks, and centrality," *Phys. Rev. E, Stat. Phys. Plasmas Fluids Relat. Interdiscip. Top.*, vol. 64, no. 1, Jun. 2001, Art. no. 016132.
[21] M. E. J. Newman, "A measure of betweenness centrality based on random walks," *Soc. Netw.*, vol. 27, no. 1, pp. 39–54, 2005.
[22] T. Opsahl, F. Agneessens, and J. Skvoretzc, "Node centrality in weighted networks: Generalizing degree and shortest paths," *Social Netw.*, vol. 32, no. 3, pp. 245–251, 2010.
[23] E. Rohrer. (2018). *Discharged-PC-Data/Snapshots*. [Online]. Available: https://git.tu-berlin.de/rohrer/discharged-pc-data/-/tree/master/snapshots.
[24] E. Rohrer, J. Malliaris, and F. Tschorsch, "Discharged payment channels: Quantifying the lightning Network's resilience to topology-based attacks," in *Proc. IEEE Eur. Symp. Secur. Privacy Workshops (EuroS&PW)*, Jun. 2019, pp. 347–356.
[25] I. A. Seres, L. Gulyás, D. A. Nagy, and A. Burcsi, "Topological analysis of bitcoin's lightning network," in *Mathematical Research for Blockchain Economy*. Budapest, Hungary: Eötvös Lorand Univ., 2020, pp. 1–12.

LUIS E. OLEAS-CHÁVEZ received the B.S. degree from the Escuela Politécnica del Ejército, Quito, Ecuador, in 2008, and the M.S. degree in computer science from Washington State University, Pullman, WA, USA, in 2014. He is currently pursuing the Ph.D. degree in computer science with the Department of Information and Communications Engineering (dEIC), Universitat Autònoma de Barcelona (UAB). He held a Senescyt Grant, in 2012. His research interests include computer security, cryptography, and distributed systems especially in blockchain technology and cryptocurrencies.

CRISTINA PÉREZ-SOLÀ received the joint Ph.D. degree from the Department of Information and Communications Engineering (dEIC), Universitat Autònoma de Barcelona, and the Computer Security and Industrial Cryptography Group (COSIC), Katholieke Universiteit Leuven. She is currently a Lecturer at the Universitat Oberta de Catalunya, where she studies Bitcoin, cryptocurrencies, and secure protocols on top of blockchain-based cryptocurrencies. Her research interests include blockchain-based cryptocurrencies and privacy in networked scenarios. Apart from cryptocurrencies and privacy, she is also interested in machine learning (specifically for relational domains and in adversarial settings), cryptography, and graph theory.

JORDI HERRERA-JOANCOMARTÍ graduated in mathematics from the Universitat Autònoma de Barcelona (UAB), in 1994. He received the Ph.D. degree from the Universitat Politècnica de Catalunya, in 2000. In 2000, he joined the Universitat Oberta de Catalunya and founded the KISON Research Group, where he is currently an External Researcher. He is also an Associate Professor with the Department of Information and Communications Engineering, UAB. He is a member of the SENDA Research Group, UAB. His research interests include privacy, computer security, and cryptography with special dedication to blockchain technology and cryptocurrencies.